Resonance Based Discrimination of Stealth Targets Coated with Radar Absorbing Material (RAM)

Sathyamurthy Anuradha[1, *] and Jyothi Balakrishnan[2]

Abstract—For the first time, a real sized complex target that is coated with an absorber material is discriminated from the uncoated one using an aspect independent discrimination method based on natural resonances. This resonance based technique provides a real-time, accurate and aspect independent solution for stealth target discrimination. First, the discrimination is studied for a complex shaped aircraft of electrical size 1.5λ. The Perfectly Electrically Conducting (PEC) target is coated uniformly with sintered nickel-zinc-ferrite, a magnetic Radar Absorbing Material (RAM) with complex dielectric and magnetic properties. The resonant range Radar Cross Section (RCS) of the aircraft for different coating thicknesses is computed using the Method of Moments (MoM). The resonances contained in the RCS are extracted using the vector fitting method, and the dominant resonances representing the target are determined by applying the power criteria. The variation in the pole placements with the increasing coating thickness is also studied. A one number quantifier of discrimination — "Risk" in dB is defined to express the amount of mismatch between the compared targets. Further, the discrimination technique is also studied for an aircraft of electrical length, 7λ. A Risk value of $2\,\mathrm{dB}$ and more is obtained in this study at all aspects. This demonstrates the capability of the algorithm to discriminate between targets of identical structure but with different material compositions.

1. INTRODUCTION

A stealth target avoids detection by enemy radars by reducing its Radar Cross Section (RCS). A number of RCS reduction (RCSR) techniques are employed which are broadly classified as active RCSR and passive RCSR [1]. Active RCSR techniques involve cancelling the radar echoes suitably at the target by employing active devices [2]. One of the passive techniques used to reduce the RCS of a target is the distributed loading [3]. It involves coating the surface of the aircraft with a radar absorbing material (RAM) that has high loss factor. However, a particular RAM is generally effective in absorbing only certain frequencies that it is designed for. Although RCSR provides stealth to the targets at far-off distances, they are not completely undetectable in the closer ranges [4]. Within the region where the stealth aircraft can be detected, a real-time, non-cooperative identification system which is automatic and accurate is indispensable for initiating appropriate countermeasure/s. In this context, the discrimination of targets that are coated with absorber from their uncoated counterparts is of practical interest in today's warfare scenario which is the main focus of this paper.

The two vital requirements of an automatic and real-time target discrimination system are: 1. The system should involve very little time for drawing accurate results, and 2. The technique should be capable of discriminating the target irrespective of the direction from which it is viewed, i.e., it should be an aspect independent process.

In resonance based discrimination techniques, the natural resonant frequencies (NRFs) contained in the late time returns of the target form the target features. NRFs are the most suited features for target discrimination as they are aspect independent by nature while their values are influenced by the size, shape, and composition of the target. This has been mathematically formulated as the Singularity Expansion Method (SEM) by Baum et al. [5]. Based on SEM formulation, a discrimination technique utilizing the natural resonances of the targets is developed in [6, 7]. The method is found to be effective in discriminating the targets whose structural features match very closely but with minor variations. The technique is found to be successful in discriminating canonical as well as complex shape conducting targets of both electrically small and large targets. In [8], two large, real sized PEC F5 aircraft with and without missiles are discriminated successfully by implementing this technique.

In the case of stealth targets coated with an absorber, the variation of resonance poles due to composition variation forms the basis for the target discrimination. The dielectric properties of absorber material are frequency dependent, and hence, the RCS reduction varies for different frequencies. The attenuation of electromagnetic energy within the absorber material depends on factors such as electric conductivity, dielectric loss, and penetration depth [9]. Therefore, the coating thickness influences the amount of dissipation of the incident electromagnetic energy. A number of papers are available in literature to understand the scattering mechanisms of a coated conducting body. These researchers have studied the influence of the variation in thickness and dielectric constant of the coating on the pole patterns in the complex-frequency plane for dielectrically-coated spheres [10–12]. It is demonstrated that the frequency and the magnitudes of RCS are altered with the coating material property and coating thickness. The changes in the permittivity and thickness of the coating on conducting cylinders are analysed using the E-pulse technique in [13]. Wierzba and Rothwell have also used the E-pulse method to study the changes in the material properties of a coated conducting cylinder with varying curvature and coating thickness [14]. The E-pulse technique with a nonplanar interrogation field is used to determine the material variations in [15]. It is shown that the variation in the dielectric constant has more impact on the damping ratios, and the variation in coating thickness influences the pole frequencies. A similar study of the effect of permittivity and coating thickness on poles and quality factor of the poles is reported in [16, 17]. The resonance poles are shown moving closer to the vertical axis, and the quality factor increases with the thickness and the relative permittivity of the coating. These published results endorse the fact that the poles are sensitive to the material properties as well as the thickness of the absorber. Thus, the natural poles of a target form the best suited features for discriminating targets with different material compositions.

In this study, it is proposed to study the efficacy of the resonance based discrimination technique developed in [6, 7] to discriminate targets that are structurally the same but with different material compositions. In order to implement this, a sintered nickel-zinc-ferrite RAM with complex dielectric and magnetic properties is used to coat the PEC target uniformly on its surface. First, the discrimination technique is applied to distinguish 1.5λ aircraft model with and without absorber coating by determining the 'Risk' defined to quantify the discrimination. Simultaneously, the variation in the pole locations of the coated aircraft for different thicknesses of absorber coating is also studied. The poles of the aircraft are extracted from their frequency domain RCS using the Vector Fitting algorithm [18]. As a second example, the discrimination technique is applied to distinguish coated and uncoated, bigger aircraft model which is a near representation of a real fighter aircraft, of electrical length 7λ in fuselage and 12λ wing span. The Risk is determined at various aspects to demonstrate the aspect independent discrimination capability of the technique. The RCSs of the targets considered in this study are computed using the commercially available CEM solver FEKO (ver.7) [19] run on a workstation with 16 Intel Xeon®processors, 2.30 GHz, 126 GiB memory.

Section 2 deals with a brief review on the technique used for discriminating stealth targets. In Section 3, the details of implementing the discrimination of coated bodies along with the results and discussion are presented followed by the conclusions in Section 4.

2. DISCRIMINATION TECHNIQUE

According to the singularity expansion method [5], the late time returns from the target contain the resonances that are dependent on the physical as well as the chemical composition of the target.

The late time response $r(t)$ of a target to a pulsed EM can be modelled as a sum of damped exponentials with complex natural resonances as shown in Eq. (1).

$$r(t) = \sum_{k=1}^{N} A_k e^{\sigma_k t} \cos(\omega_k t + \phi_k), \quad t > t_l \tag{1}$$

Here, t_l is the beginning of the late time response; A_k and ϕ_k are the aspect dependent amplitude and phase of the kth mode, $s_k = -\sigma_k \pm j\omega_k$, respectively; and N modes are assumed to be excited by the incident wave. SEM considers the response as that of a linear time-invariant system whose response can be represented in the s-domain as a transfer function modelled with simple poles as shown in Eq. (2).

$$R(s) = \sum_{k=1}^{2N} \frac{C_k}{s - s_k} \tag{2}$$

Since the natural frequencies are independent of excitation while depending upon the detailed size, shape, and composition of the target, these frequencies are unique representations of a target which form the basis for target discrimination implemented in this study.

In this study, the natural resonant frequencies of targets are extracted from the late time returns by using the Vector Fitting method [18]. The discrimination method is explained here briefly for the sake of completeness. The 'd' dominant NRFs, s_d of known target are identified using the criteria described in [7] and are used to construct the distinction polynomial $D(j\omega) = \prod_d (j\omega - s_d)$ which forms the database of the known target. The RCS $A(\omega)$ of the stealth (unknown) target determined in the resonance range of $(\omega_1 - \omega_2)$ is used to determine the risk factor using Eq. (3).

$$Risk\ factor = \int_{\omega_1}^{\omega_2} \left\{ \frac{d^3}{d\omega^3} \left[|D(j\omega)|^2 \cdot A(\omega) \right] \right\}^2 d\omega \tag{3}$$

The normalized Risk in identifying the unknown target as the database (known) target is defined using Eq. (4). R_{uk} is the risk factor in identifying the unknown target as the known target, and R_{kk} is the risk factor in identifying the known target with itself.

$$Risk = \frac{R_{uk}}{R_{kk}} = \frac{\int_{\omega_1}^{\omega_2} \left\{ \frac{d^3}{d\omega^3} [|D_k(j\omega)|^2 \cdot A_u(\omega)] \right\}^2 d\omega}{\int_{\omega_1}^{\omega_2} \left\{ \frac{d^3}{d\omega^3} [|D_k(j\omega)|^2 \cdot A_k(\omega)] \right\}^2 d\omega} \tag{4}$$

In decibels, Risk is expressed as

$$Risk_{in\,dB} = 10 \log \left(\frac{R_{uk}}{R_{kk}} \right) \tag{5}$$

3. DISCRIMINATION OF RAM COATED AND UNCOATED TARGETS

3.1.a. Discrimination of 1.5λ Aircraft: with and without RAM Coating

As the first example, a PEC 1.5λ aircraft model, shown in Fig. 1, is used as the database target. The dimensions of the aircraft are presented in Table 1 [7].

3.1.b. Computation of RCS of the 1.5λ Aircraft Model

The PEC aircraft is modelled in CADFEKO [19]. The fuselage of the aircraft is aligned along the Z-direction. The monostatic RCS responses are computed using the MoM solver at different aspect angles varied from $\phi = 0°$; $\theta = [0\ 30\ 60\ 90\ 120\ 150\ 180]$ degrees, for a frequency range of 50 MHz–400 MHz at 256 discrete points. The frequency range includes the half lambda frequencies corresponding to maximum and minimum lengths of the aircraft. The frequency response of the PEC aircraft to linearly polarized signal of unit amplitude computed at different aspect angles is shown in Fig. 2.

The entire aircraft is coated uniformly with a magnetic RAM of sintered nickel-zinc-ferrite with dielectric and magnetic properties 27+j54 and 15+j45, respectively, at 100 MHz [3]. Usually the
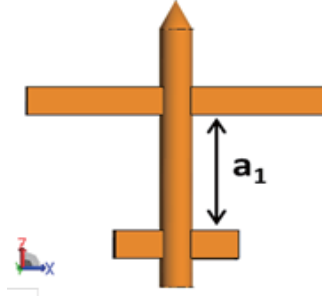
Figure 1. 1.5λ aircraft model.

Table 1. Dimensions of 1.5λ aircraft model.

Parameters	Value in meters
Length of aircraft	1
Length of front wing	0.92
Length of back wing	0.38
Distance $\mathbf{a_1}$	0.4
Placement of front wing from head	0.2
Width of the wings	0.1
Thickness of wings	0.05
Radius of cylinder	0.05
Cone height	0.1
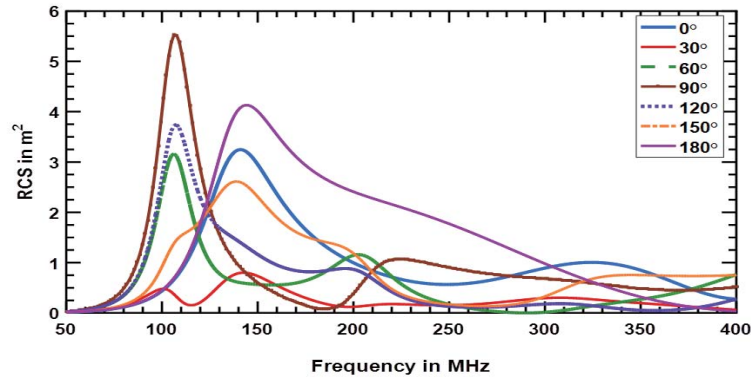
Figure 2. RCS response of 1.5λ aircraft model (PEC).

electrical and magnetic properties of the absorber are specified at a particular frequency. The maximum reduction in RCS is achieved when the coating thickness is of the order of quarter wavelength [20] corresponding to the frequency specified. Therefore, the discrimination is carried out for the coating thickness when the absorption is most effective. The EDITFEKO feature is used to set the material properties of the coating using the CO card [19]. The RCS of the coated aircraft was computed for four different coating thicknesses 'tc' of 1 mm, 5 mm, 10 mm, and 14.02 mm ($tc = 14.02$ mm corresponds to the thickness for which maximum absorption occurs at 100 MHz). The frequency response of the coated aircraft is computed similar to the PEC counterpart at the aspect angles ranging from [$\theta = 90$; $\phi = 0, 30, 60, 90, 120, 150, 180$] degrees at 256 discrete frequencies between 50 MHz and 400 MHz.
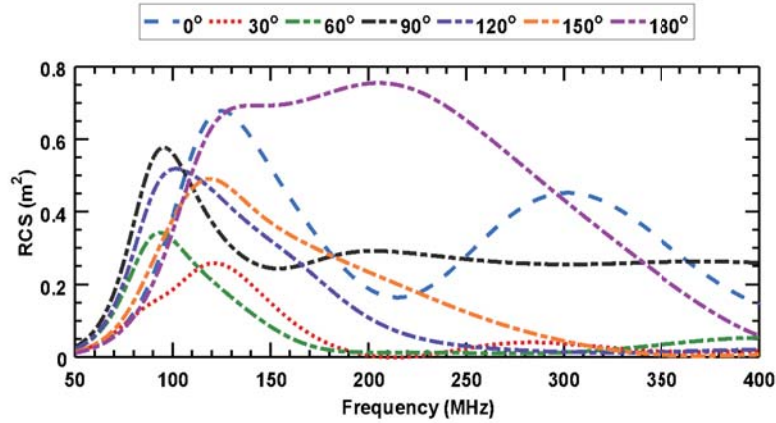
Figure 3. RCS of coated 1.5λ aircraft ($tc = 1\,\text{mm}$).
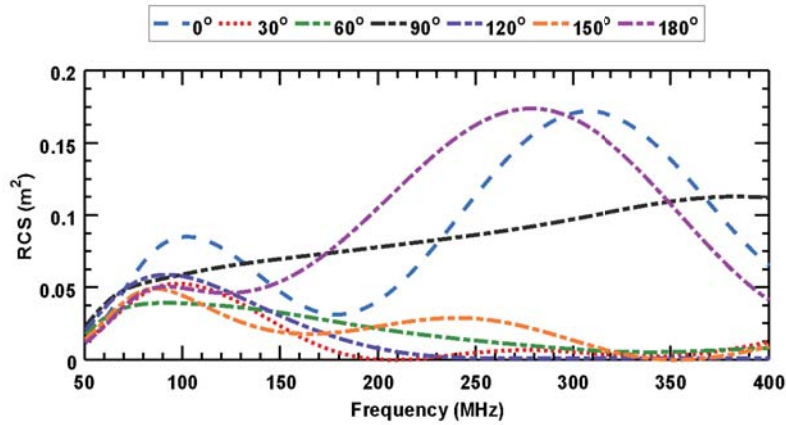
Figure 4. RCS of coated 1.5λ aircraft ($tc = 5\,\text{mm}$).

The frequency responses of the coated aircraft for different coating thicknesses are shown in Figs. 3–6. As expected, it is observed that the overall amplitudes are drastically reduced with the increase in coating thickness irrespective of the aspect angle. Also, the RCS reduction is maximum at 100 MHz in accordance with the absorber specification. The RCS has maximum reduction ($< 0.03\,\text{m}^2$) at 100 MHz in the case of $tc = 14.02\,\text{mm}$ (Fig. 6).

3.1.c. Determination of the NRFS OF 1.5λ Aircraft

Discrimination of aircraft with and without coating requires the computation of dominant NRFs of the database target alone, which is the PEC aircraft (without RAM coating). However, it is interesting to understand the variations in the pole locations of the coated aircraft for different coating thicknesses and compare them with that of the uncoated PEC aircraft. The dominant NRFs of the aircraft with different coating thicknesses are determined by extracting VF poles from the frequency response data and selecting those poles as the dominant poles whose power contribution to the signal is more than 10% of the total power in the signal [7]. The dominant poles of coated aircraft with different thicknesses and the PEC aircraft poles determined are plotted in Fig. 7. Although the resonant poles are complex conjugates, only the left half of s-plane (LHP) poles with positive imaginary parts are shown in the figure. The approximate loci, along which the poles of PEC and coated aircraft with different coating thicknesses lie, are indicated with dashed lines. The cosine of the angle between the negative real axis and the loci determines the damping ratio. The damping ratio indicates the rapidity in the decay of oscillations. The lines are marked with the same colours as that used to indicate the poles of a particular
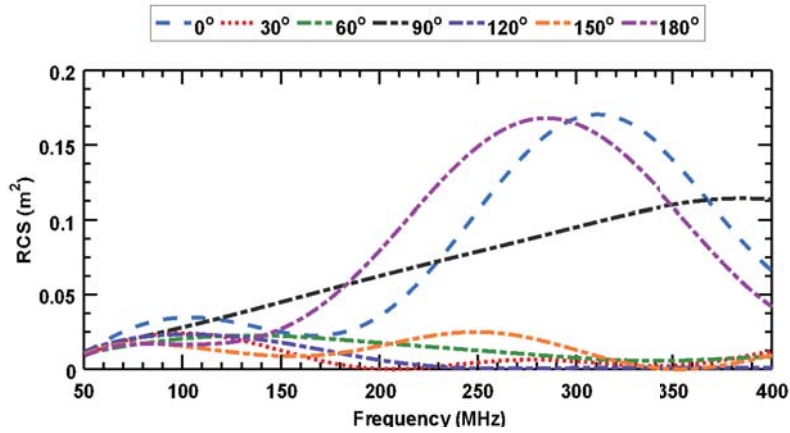
Figure 5. RCS of coated 1.5λ aircraft ($tc = 10\,\text{mm}$).
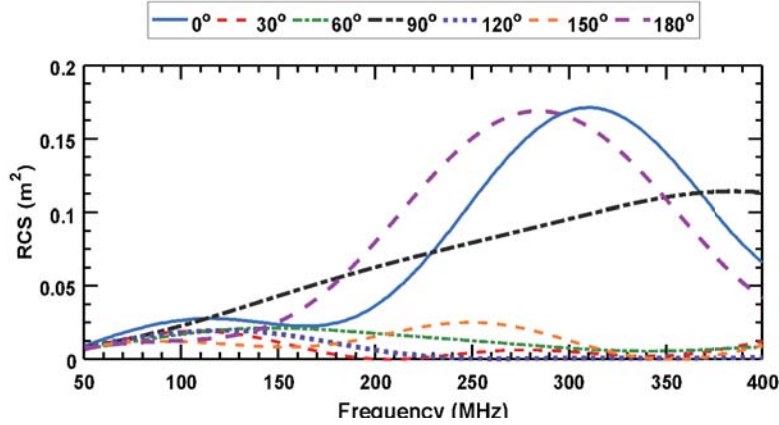
Figure 6. RCS of coated 1.5λ aircraft ($tc = 14.02\,\text{mm}$).
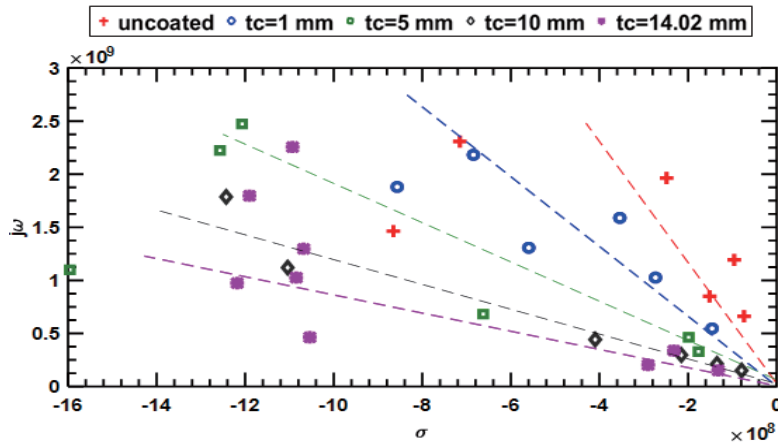
Figure 7. Dominant poles of 1.5λ aircraft — uncoated and coated (different thickness).

aircraft. The damping ratio along the imaginary axis is minimum ($\cos(90°)$) and maximum along the negative real axis ($\cos(0°)$). It is observed in Fig. 7 that, as the coating thickness is increased, the poles of the aircraft are relocated towards the loci of higher damping ratios. The EM wave is damped or absorbed effectively when the coating thickness is of quarter wavelength.

3.1.d. Discrimination Results

The PEC 1.5λ aircraft (uncoated) model is chosen to be the database target whose dominant poles are used to build the distinction polynomial. The PEC target is discriminated against the 1.5λ aircraft model applied with RAM coating. The RCSs of these coated targets are used to quantify the amount of mismatch at aspect angles [$\theta = 90°$; $\phi = 0°$, 30°, 60°, 90°, 120°, 150°, 180°] using the definition of Risk. The Risk in dB is determined, and the results are presented in Table 2.

Table 2. Discrimination of coated and uncoated 1.5λ aircraft.

Aspect angle	Risk in dB			
in degrees	$tc = 1\,\text{mm}$	$tc = 5\,\text{mm}$	$tc = 10\,\text{mm}$	$tc = 14.02\,\text{mm}$
0	8.0274	12.9471	13.1190	13.0899
30	−0.6274	9.9493	16.6865	18.6280
60	−3.7459	−1.2054	3.7892	4.2853
90	13.4644	20.3333	20.3435	20.3413
120	−5.7942	−10.7076	−3.0142	−1.5777
150	−25.1413	−3.4500	2.6602	2.5894
180	19.5524	29.2579	29.6724	29.6231

More than 2 dB of 'Risk' value (in magnitude) obtained at most of the aspects for a target is a clear indication of the dissimilarity. At 30° aspect, in the case of discriminating 1 mm coated aircraft, the value of Risk is below 1 dB. This may be viewed as the aspect at which the RCSs of the coated and uncoated aircraft contain closely resembling poles causing maximum pole cancellation in the risk factor and eventually leading to a lower Risk value. In such cases where the risk value is less than 2 dB in magnitude, it may be stated that the final discrimination judgement should be arrived only after assessing the Risk value at more than one aspect. The discrimination results obtained demonstrate the ability of the discrimination technique to distinguish targets that differ in material composition.

3.2.a. Discrimination of a 7λ PEC Aircraft with and without RAM Coating

As the second example for discrimination of targets with composition variation, a model PEC aircraft of 7λ fuselage, 12λ wing span, and height of 2λ, shown in Fig. 8, is used as the database aircraft. It is used to represent a scaled model of typical fighter aircraft Me163B-1. Though the model is not an exact replica of the real aircraft, it is used for the analysis purpose.
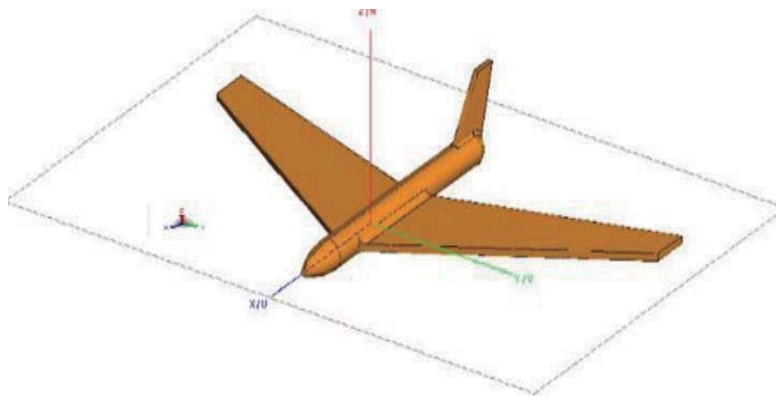
Figure 8. 7λ PEC aircraft model.

3.2.b. Computation of RCS of the 7λ Aircraft Model

The RCS of the PEC aircraft was computed using MoM at seven different aspect angles ranging from $\theta = 90°$; $\phi = [0, 30, 60, 90, 120, 150, 180]$ degrees. The response at each aspect was computed using the MoM solution for a frequency range of 1 MHz to 500 MHz. This range covers the half-lambda rule to include the minimum and maximum characteristic dimensions of the aircraft for proper resonance region response. Between 1 MHz and 500 MHz, the RCS is computed at 64 discrete points. The PEC aircraft was coated uniformly with the same RAM material used in the previous case and $tc = 14.02$ mm. The simulations were carried out on a system with 16 Intel Xeon®processors, 2.30 GHz, 126 GiB memory. The simulations were run on a single processor with 12 cores. The simulation time and memory requirement for the RCS computations of uncoated and coated aircraft are given in Table 3.

Table 3. Simulation comparison of coated and uncoated 7λ aircraft.

Parameters	Uncoated	Coated
No. of meshes	22046	22046
No. of unknowns	33069	33069
CPU time in hours	81.406	561.650
Peak memory in GB	8.303	8.343

It may be noted that the computation time required for the coated aircraft is seven times of that of the uncoated one. The number of unknowns and the memory required remain almost the same in both the cases.

The RCSs of the uncoated and coated aircraft are shown in Figs. 9 and 10, respectively. A comparison of the two plots shows the impact of the RAM coating on the RCS of the aircraft. The magnitude of the RCS has been reduced by almost 30 dB at the broad-side incidence.
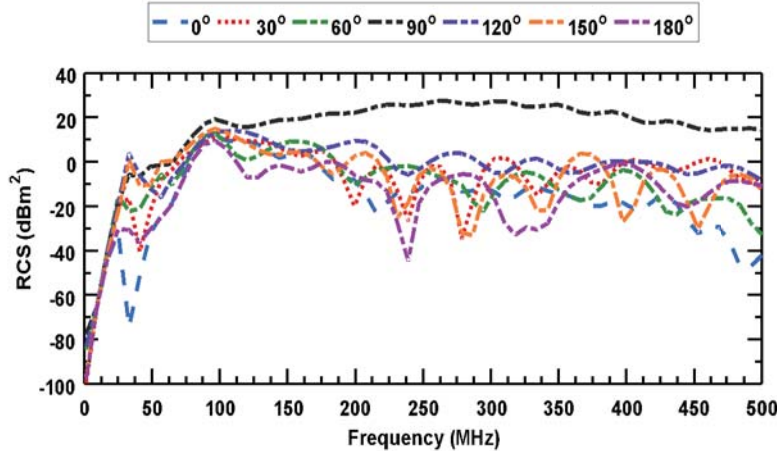
Figure 9. RCS of PEC 7λ aircraft (uncoated).

3.2.c. Determination of NRFs of Coated and Uncoated 7λ Aircraft

The RCS plots show a lot of resonant peaks in the computed range of frequency. This indicates that a large number of poles are representative of the target in the resonant range. The order N of the function was determined to be around 50 at all aspects for a better convergence of the poles using the VF method, and the RMSE was 5.57E-7 at 0° aspect. From the set of 50 poles, the most dominant NRFs useful for discrimination were determined based on the power contribution criteria and are presented in Fig. 11.

The plot clearly shows the variation in the pole values caused by the RAM coating. Similar to the pole relocation observed in the case of 1.5λ aircraft for change in material composition, the poles of the coated aircraft have moved far into the LHP indicating higher values of damping ratio.
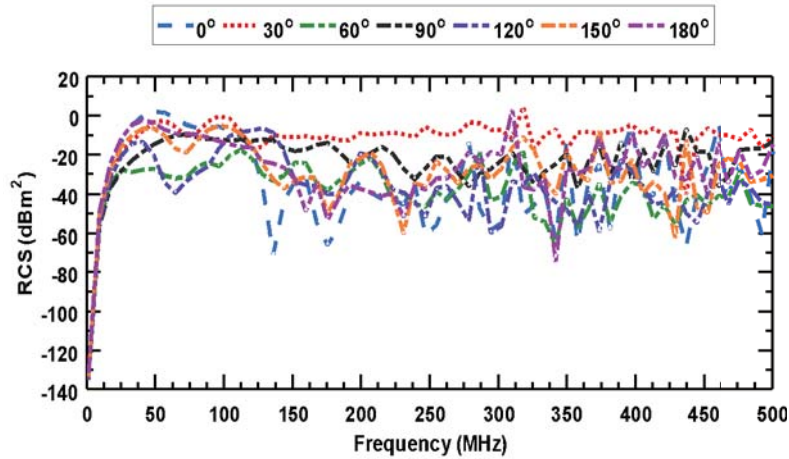
Figure 10. RCS of 7λ aircraft coated with RAM ($tc = 14.02\,\text{mm}$).
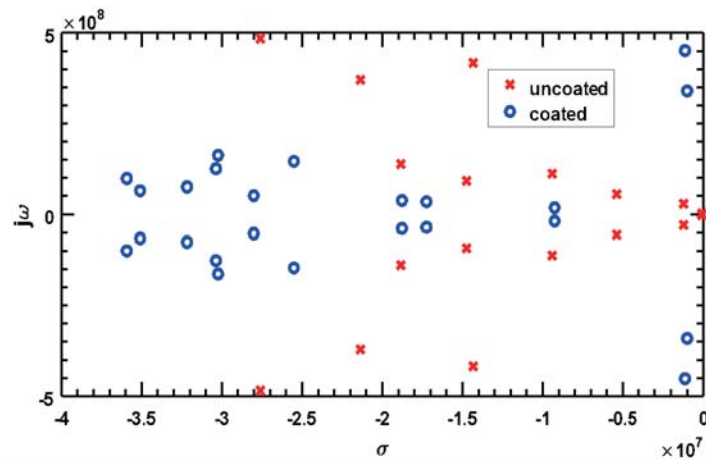
Figure 11. Dominant NRFs of uncoated and coated 7λ aircraft.

Table 4. Discrimination of uncoated and coated 7λ aircraft model.

Aspect angle in degrees	Risk in dB
0	30.0565
30	2.6842
60	15.0455
90	6.0800
120	-14.2059
150	3.3739
180	3.7763

3.2.d. Discrimination Results

The distinction polynomial was built using the dominant poles of the uncoated aircraft which is considered as the database target. The Risk values obtained at various aspects are tabulated in Table 4. The value of Risk is found to be greater than 2 dB in magnitude at all aspects. This demonstrates the capability of the algorithm to discriminate effectively the large sized targets with composition variation.

4. CONCLUSIONS

The main focus of this paper was to apply the discrimination technique to the problem of distinguishing the absorber coated and uncoated aircraft which find application in countering stealth aircraft. For the examples studied, the Risk value of more than 2 dB is achieved at all aspect angles which clearly demonstrates the aspect independent discrimination capability of the technique to discriminate targets with different material compositions. In addition, the pattern in the variation of dominant poles of coated aircraft with the coating thickness has been analyzed by studying the damping ratio pattern. The damping ratio is seen to increase with the coating thickness.

The main advantage of the technique used here is that the direct amplitude returns of the target is sufficient for the discrimination purpose and does not require any processing stage to extract the features from the target echo. It also provides a one number description for discrimination called as 'Risk'. Another key advantage of the technique is the aspect independent discrimination capability. These key features of the discrimination algorithm make it suitable for real time implementation. This technique may also be employed in some commercial applications such as to determine the degradation of a coating (paint) on a material due to factors like aging or prolonged use.

Nevertheless, the latest technique in stealth is to employ nanomaterials for stealth purposes [21]. In the event of nanomaterial coated bodies exhibiting prominent pole variations, the technique could still prove its efficiency that may be further studied.

ACKNOWLEDGMENT

REFERENCES

1. Zaker, R. and A. Sadeghzadeh, "Passive techniques for target radar cross section reduction: A comprehensive review," *International Journal of RF and Microwave Computer-Aided Engineering*, Vol. 30, 2020, https://doi.org/10.1002/mmce.22411.
2. Sengupta, S., H. Council, D. R. Jackson, and D. Onofrei, "Active radar cross section reduction of an object using microstrip antennas," *Radio Science*, Vol. 55, 2020, https://doi.org/10.1029/2019RS006939.
3. Knott, E. F., J. F. Schaeffer, and M. T. Tuley, "Radar cross section," *SciTech*, 2004.
4. Zikidis, K., A. Skondras, and C. Tokas, "Low observable principles, stealth aircraft and anti-stealth technologies," *Journal of Computations & Modelling*, Vol. 4, No. 1, 2014, 129–165, ISSN: 1792–7625 (print), 1792–8850 (online), Scienpress Ltd., 2014/
5. Baum, C. E., E. J. Rothwell, Y. F. Chen, and D. P. Nyquist, "The singularity expansion method and its application to target identification," *Proceedings of the IEEE*, Vol. 79, No. 10, 1481–1492, Oct. 1991.
6. Anuradha, S. and J. Balakrishnan, "Discrimination of closely resembling PEC targets based on natural resonant frequencies," *IEEE-MTT International Microwave And RF Conference (IMARC)*, Bengaluru, Dec. 2014.
7. Anuradha, S. and J. Balakrishnan, "Resonance based discrimination of targets with minor structural variations," *2016 Asia-Pacific Microwave Conference (APMC)*, New Delhi, 2016.

8. Anuradha, S. and J. Balakrishnan, "Radar target discrimination of real size aircraft with minor structural variations: Challenges and solutions," *Progress In Electromagnetics Research C*, Vol. 102, 139–148, 2020.

9. Luiza de C., F., M. A. Alves, and M. C. Rezende, "Microwave absorbing paints and sheets based on carbonyl iron and polyaniline: measurement and simulation of their properties," *Journal of Aerospace Technology and Management*, Vol. 2, No. 1, 63–70, 2010.

10. Rao, S. M., C.-C. Cha, R. L. Cravey, and D. L. Wilkes, "Electromagnetic scattering from arbitrary shaped conducting bodies coated with lossy materials of arbitrary thickness," *IEEE Transactions on Antennas and Propagation*, Vol. 39, 627–631, May 1991.

11. Analoui, M. and Y. Kagawa, "Electromagnetic scattering from conductor-coated material bodies," *International Journal of Numerical Modelling: Electronic Networks, Devices and Fields*, Vol. 4, No. 4, 287–299, 1991.

12. Howell, W. E. and H. Uberall, "Complex frequency poles of radar scattering from coated conducting spheres," *IEEE Transactions on Antennas and Propagation*, Vol. 32, No. 6, 624–627, Jun. 1984.

13. Vollmer, H. and E. J. Rothwell, "Resonance series representation of the early-time field scattered by a coated cylinder," *IEEE Transactions on Antennas and Propagation*, Vol. 52, No. 8, 2186–2190, Aug. 2004.

14. Wierzba, J. F. and E. J. Rothwell, "E-pulse diagnostics of curved coated conductors with varying thickness and curvature," *IEEE Transactions on Antennas and Propagation*, Vol. 54, No. 9, 2672–2676, Sept. 2006.

15. Rothwell, E. J. and G. D. Dester, "E-pulse diagnostics of a coated conductor using a nonplanar interrogation field," *IEEE Transactions on Antennas and Propagation*, Vol. 57, No. 2, 587–590, Feb 2009.

16. Chantasen, N., A. Boonpoonga, and S. Burintramart, "Radar target identification of coated object using Cauchy method," *IEEE Conference on Antenna Measurements & Applications (CAMA)-2015*, 1–3, Chiang Mai, 2015.

17. Chauveau, J., N. de Beaucoudrey, and J. Saillard, "Modification of resonance poles of a conducting target by a dielectric coating," *2007 European Radar Conference*, 440–443, Munich, 2007.

18. Gustavsen, B. and A. Semlyen, "Rational approximation of frequency domain responses by vector fitting," *IEEE Trans. Power Delivery*, Vol. 14, No. 3, 1052–1061, Jul. 1999.

19. FEKO Suite 7 User Manual, EM Software and Systems (EMSS), 2014.

20. Raju, A. U., "Radar cross section (RCS) analysis of complex shaped radar absorbing material (RAM) coated bodies," Bengaluru, May 2013 (Thesis).

21. Kolanowska, A., D. Janas, A. P. Herman, R. G. Jęrysiak, T. Giżwski, and S. Boncel, "From blackness to invisibility — Carbon nanotubes role in the attenuation of and shielding from radio waves for stealth technology," *Carbon*, Vol. 126, 31–52, 2018, ISSN 0008-6223, https://doi.org/10.1016/j.carbon.2017.09.078.